PROCEEDINGS OF THE INTERNATIONAL CONFERENCE
NANOMATERIALS: APPLICATIONS AND PROPERTIES
Vol. **2** No 2, 02FNC18(4pp) (2013)

Kinetics of Nickel Particles Nucleation and Growth from the Serine-Containing Electrolyte

L.V. Sapronova*, N.V. Sotskaya†, O.V. Dolgikh‡,

Voronezh State University, 1, Universitetskaya Sq., 394006 Voronezh, Russia

(Received 10 June 2013; published online 02 September 2013)

Kinetics of nickel particles nucleation and growth from the serine-containing electrolyte was studied by cyclic voltammetry and chronoamperometry. It was shown, that the initial stage of nickel electrodeposition onto a polycrystalline copper electrode conforms to instantaneous nucleation mechanism. Main parameters of nucleation process (diffusion coefficients, number of active sites, nucleation rate, formation work of critical cluster and its size) were calculated. Partial curves of nickel deposition and hydrogen evolution were obtained.

Keywords: Nickel, Electrocrystallization, Kinetics, Modelling.

PACS number: 81.15.Pq

1. INTRODUCTION

In electrodeposition processes, initial stages of new phase formation significantly influence the structure, physico-chemical and catalytic properties of the coating. It matters much to production of thin and ultrathin nickel films [1-3]. In [4] instantaneous nucleation with a 3D diffusion-controlled growth was determined by Scharifker–Hills' theoretical model for the process of nickel electrocrystallization from dilute simple sulfate solutions. But in complex nickel solution data depend on many factors such as ligand's nature, electrolyte composition, especially anions, influencing the overpotential due to both complexation and adsorption [1, 2, 5].

Complex nickel solutions containing nontoxic ligands, for instance amino acids, are most promising. Their application allows to increase considerably lability of inner coordination sphere of complexes, to occur the process in media close to neutral [5-7]. Thus, the aim of this work is study of kinetics of nickel particles nucleation and growth from electrolyte containing 2-amino-3-hydroxypropanoic acid (serine).

2. EXPERIMENTAL

Investigations were carried out in electrolyte containing 0.08 mol/l $NiCl_2$ and 0.20 mol/l serine (HSer) at pH 5.5. Solutions were prepared from chemically grade reagents, and doubly distilled water. Required pH was reached by adding 10% NaOH solution and controlled by an EV-74 universal ionometer (accuracy±0.05).

Electrochemical studies were performed using IPC-Compact potentiostatic complex in the standard three-electrode cell with. Polycrystalline copper working electrode (S = 0.20 cm^2) was use, silver-silver chloride reference electrode and platinum-gauze counter electrode. All the potentials are given with respect to the standard hydrogen electrode. Before each experiment, the working electrode was subjected to standard mechanical treatment [3]. Cyclic voltammograms were obtained at scan rate $v = 5 \cdot 10^{-3}$ V/s. Electrochemical deposition was performed using potentiostatic method during which the current transients were recorded.

3. RESULTS AND DISCUSSION

3.1 Thermodynamic analysis

In aqueous solutions, besides aquacomplexes $[Ni(H_2O)_6]^{2+}$, the species with amino acid anions (Ser) also present, namely: $[Ni(H_2O)_4\,Ser]^+$, $[Ni(H_2O)_2\,Ser_2]^0$, $[Ni\,Ser_3]^-$ [8]. Fraction of each of these complexes (α_i)was calculated by means of thermodynamic analysis of ionic equilibriums occurring in the electrolyte under investigation. The analysis was carried out by standard procedure [9] using material balance equations with respect to nickel ions and ligands, proton equilibrium and electro-neutrality conditions. It was found that in the investigated solution, nickel ions mainly present as positive ($\alpha_{[Ni(H_2O)_4\,Ser]^+} = 0.525$) and neutral ($\alpha_{[Ni(H_2O)_2\,Ser_2]^0} = 0.373$) serine complexes. Fraction of negatively charged complexesis negligible ($\alpha_{[NiSer_3]^-} = 0.009$).

3.2 Voltammetric study

Formation of metal particle is the result of parallel discharge of complex nickel ions onto electrode surface:

$$\left[Ni\left(H_2O\right)_{6-2n}\,Ser_n\right]^{2-n} + 2\bar{e} = Ni^0, \qquad (3.1)$$

where n = 0..3. Hydrogen evolution from hydronium ions or water molecules is concurrent reaction influencing the initial stages of new phase initiation.

A voltammetric study was carried out to determine the potentials where the electrodeposit can be obtain in the electrolyte with serine. Cathodic voltammetric curve presented in Fig. 1 has a clearly pronounced peak *A*

* lynatikk@gmail.com
† nvs@chem.vsu.ru
‡ dov@chem.vsu.ru

(– 0.91 V) corresponding to the electroreduction of nickel ions. Further increase of cathodic current is observed due to the increasing contribution of hydrogen evolution reaction. During the backward potential scan, cathodic and anodic branches intersect at the potential -0.74 V (point B) indicating the transition from the mechanism of deposition without nucleation at low cathodic potentials to the formation of new phase involving a nucleating process [10, 11].

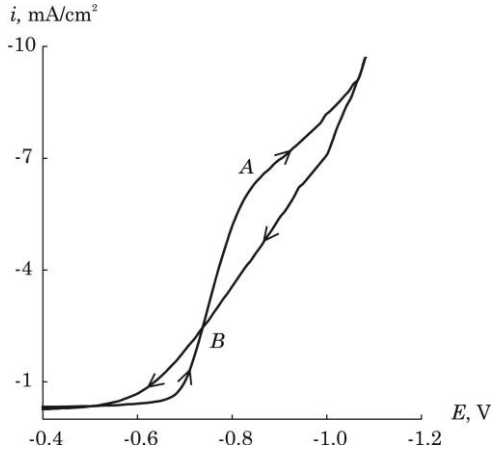

Fig. 1 – Voltammogram obtained on polycrystalline copper electrode from serine containing electrolyte (5 mV/s).

3.3 Chronoamperometric study

Current transients were obtained at given potentials to evaluate the kinetics of nickel particles nucleation and growth. Fig. 2 shows a family of potentiostatic current-time transients. All curves are characterized by the presence of current maximum (i_m) corresponding to nickel electrodeposition. Amplitide of this maximum increases with increasing cathodic potential, and the corresponding time of this maximum (t_m) decreases. The current then drops and the transient approaches that corresponding to linear diffusion to the total area of the copper electrode surface. It should be noticed that a large decaying current is also observed at the beginning of transients recorded at the potentials lower –1.09 V, due to the charging of double layer and possibly to adsorption-desorption processes [12].

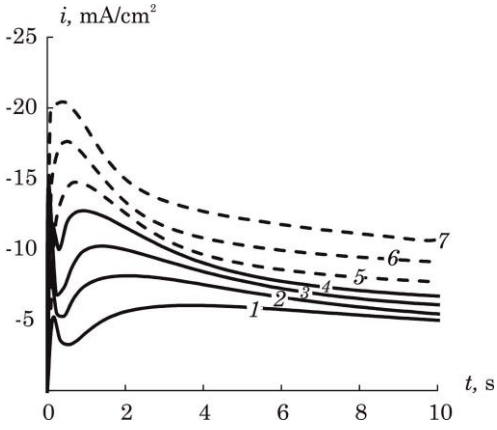

Fig. 2 – Family of potentiostatic current-time transients obtained during the nickel electrodeposition onto polycrystalline copper electrode at different potentials, V: –0.89 (1); –0.94 (2); –0.99 (3); –1.04 (4); –1.09 (5); –1.14 (6); –1.19 (7)

The curves fit closely to the behavior described by models considering multiple nucleation and diffusion-controlled growth of three dimensional nickel crystallites.

Shape of these transients doesn't significantly change with increasing of the negative potentials. At more negative step potentials, maxima on the potentiostatic curves are more pronounced.

3.4 Calculation and analysis of the kinetic parameters of nickel nucleation process

Current recorded during the potentiostatic nickel deposition is the total value (i_{total}) depending on the rate of two parallel processes. Therefore, the model proposed by authors [13] was used to describe current-time transients. The model allows to obtain partial curves of nickel deposition and hydrogen evolution by non-linear fitting of the experimental data by Eq. (3.2).

$$i_{total}(t) = \left(P_1^* + P_4 t^{-1/2}\right) \times \times \left(1 - \exp\left\{-P_2\left[t - \frac{1-\exp\left(-P_3 t\right)}{P_3}\right]\right\}\right) \quad , \qquad (3.2)$$

with $P_1^* = P_1\left(2c_0 M / \pi\rho\right)^{1/2}$; $P_1 = z_H F k_H$;

$P_2 = \left(8\pi^3 c_0 / \rho\right)^{1/2} N_0 D$; $P_3 = A$; $P_4 = 2FD^{1/2}c_0 / \pi^{1/2}$,

where $z_H F$ is the molar charge transferred during the hydrogen evolution process, k_H is the rate constant of the hydrogen evolution reaction, c_0 is the bulk concentration of the metal ion in the solution, ρ the density of the deposit, M its molar mass, N_0, A, D are the number density of active sites for nucleation on the electrode surface, the rate of nucleation and the diffusion coefficient, respectively.

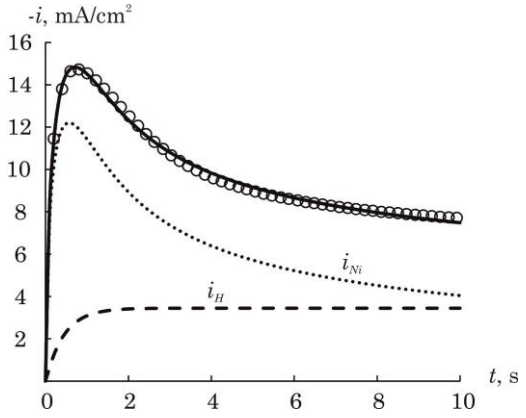

Fig. 3 – Comparison between experimental transient (○) obtained during nickel deposition at $E = -1.09$ V and the theoretical current transient (—) after non-linear fitting of the experimental data by Eq. (3.2) With following parameters: $P_1^* = 3.44$ mA cm^{-2}, $P_2 = 2.27$ s^{-1}, $P_3 = 65.24$ s^{-1}, and $P_4 = 12.78$ mA cm^{-2} s$^{1/2}$. The individual contributions to the total current due to nucleation process (i_{Ni}) and to hydrogen evolution (i_H) are also shown

Fig. 3 shows a comparison of the experimental transient obtained during nickel electrodeposition onto polycrystalline copper electrode at $E = -1.09$ V and theoretical current transient after non-linear fitting of the

experimental data by Eq. (3.2) to. Parameters of nickel nucleation process such as A, N_0, D, and k_H were calculated from P_1^*, P_2, P_3, P_4 parameters obtained by iterative procedure.

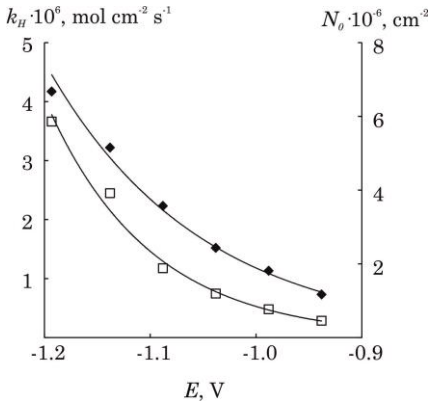

Fig. 4 – Rate constant of hydrogen evolution reaction (k_H, ♦) and the number density of active sites for nucleation on the electrode surface (N_0, □) as functions of potential

It can be seen from Fig. 4 that k_H and N_0 values increase with increasing cathodic potential. Average value of the nickel ion diffusion coefficient of $(1.87\pm0.33)\cdot10^{-6}$ cm^2 s^{-1} was found as the result of calculation.

The work of formation of the critical nucleus (ΔG^*) and its size (n^*) were calculated from the slope of ln ($A\exp(azFE/RT)$) vs. E^{-2} dependence (see Fig. 5 – inset) by the following equations [14, 15]:

$$\Delta G^* = -\frac{RT}{E^2}\cdot\frac{d\ln\left(A\exp\left(\alpha zFE/RT\right)\right)}{dE^{-2}}, \quad (3.3)$$

$$n^* = \frac{2\Delta G^*}{zFE}, \quad (3.4)$$

with an nickel ion transfer coefficient $\alpha = 0.5$. Fig. 5 presents the dependence ΔG^* on E^{-2}. Obtained by the Eq. (3.4) the number of atoms in the critical nucleus is less than 1. The meaning of this result is that within the investigated potential range the thermodynamic barrier for nucleus formation is close to zero and only the kinetics determine the nucleation rate constant A on the polycrystalline copper surface. Thus, it appears that each nickel atom adsorbed on an active site is a stable 'cluster' which can grow irreversibly at the given potential [16].

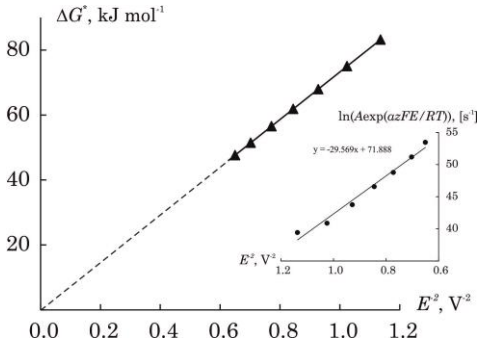

Fig. 5 – ΔG^* of formation of nickel nucleus as a function of E^{-2}. Inset: in ln ($A\exp(azFE/RT)$) vs. E^{-2} plots of nucleation rate constants obtained from analysis of current transients with Eq. (3.2)

On the basis of the values P_1^*, P_2, P_3, P_4 obtained from the best-fit of the experimental data the partial currents of nickel deposition (i_{Ni}) and hydrogen evolution (i_H) presented on Fig. 3 were estimated by following equations:

$$i_{Ni}(t) = P_4 t^{-1/2}\theta(t), \quad (3.5)$$

$$i_{Ni}(t) = P_1^*\theta(t), \quad (3.6)$$

where $\theta(t) = \left(1-\exp\left\{-P_2\left[t-\left(1-\exp\left(-P_3 t\right)\right)/P_3\right]\right\}\right)$ is the fraction of the electrode surface covered by 2D diffusion zones [13].

Partial curves of nickel deposition were compared with the theoretical expressions in normalized coordinates for instantaneous (Eq. (3.7)) and progressive (Eq. (3.8) nucleation as limiting cases [12].

$$\left(\frac{i}{i_m}\right)^2 = 1.9542\left(\frac{t}{t_m}\right)^{-1}\cdot\left\{1-\exp\left[-1.2564\left(\frac{t}{t_m}\right)\right]\right\}^2 \quad (3.7)$$

$$\left(\frac{i}{i_m}\right)^2 = 1.2254\left(\frac{t}{t_m}\right)^{-1}\cdot\left\{1-\exp\left[-2.3367\left(\frac{t}{t_m}\right)\right]\right\}^2 \quad (3.8)$$

It is clear from Fig. 6 that the nickel deposition on the polycrystalline copper substrate from serine-containing electrolyte follows closely the theoretical response for instantaneous nucleation at potentials under study.

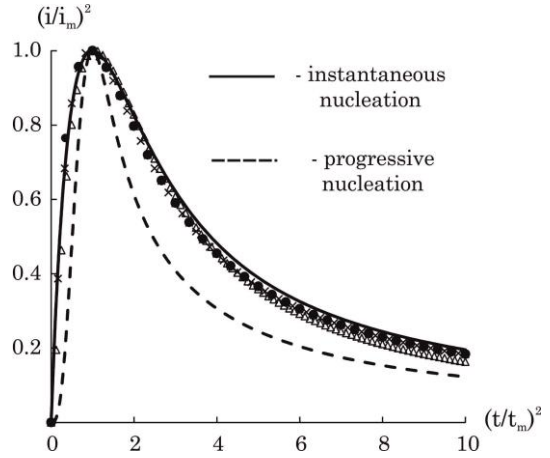

Fig. 6 – Comparison between the theoretical nondimensional plots for instantaneous (Eq. (3.7)) and progressive (Eq. (3.8)) nucleation and partial curves of nickel deposition at different potentials, V: –0.94 (Δ); –1.09 (×); –1.19 (●)

The average diffusion coefficient of Ni^{2+} species of $(1.97\pm0.41)\cdot10^{-6}$ cm^2 s^{-1} was also calculated from partial curves of nickel deposition by following equation [12]:

$$D = \frac{i_m^2\cdot t_m}{0.1629\left(zFc_0\right)^2}. \quad (3.9)$$

This value is close to that obtained by model [13]. For comparison, diffusion coefficient of nickel ions was estimated by Eq. (3.9) using total potentiostatic curves (Fig. 2). In this case the diffusion coefficient was over-

stated and equal to $(4.09\pm0.86)\cdot10^{-6}$ cm^2 s^{-1} due to the presence of the side hydrogen evolution reaction.

4. CONCLUSION

It was shown that the initial stage of nickel electrodeposition onto a polycrystalline copper electrode from serine-containing electrolyte involves the process of instantaneous nucleation and growth of the stable nickel cluster under diffusion-controlled condition. Main characteristics of nickel nucleation such as the diffusion coefficient of Ni^{2+}, number density of active sites for nucleation on the electrode surface, the rate of nucleation, the work of formation of the critical nucleus and its size were calculated. Contribution of hydrogen evolution reaction to the nickel electodeposition process was estimated. The partial curves of nickel deposition and hydrogen evolution were obtained.

REFERENCES

1. M. Toradi, A. Dolati, *J. Appl. Electrochem*. **40**, 1941 (2010).
2. D. Grujicic, B. Pesic, *Electrochim. Acta*. **51** №13, 2678 (2006).
3. O.V. Dolgikh, N.V. Sotskaya, Vu Thi Duyen, E.A. Kotlyarova, B.L. Agapov, *Protection of metals and physical chemistry of surfaces*. **45** №6, 718 (2009).
4. S.M. Janjan, F. Nasirpouri, M.G. Hosseini, *Russian journal of electrochemistry*. **47** №7, 787 (2011).
5. A. Sahari, A. Aziz, G. Schmerber, A. Dinia, *Surface review and letters*. **15** №6, 717 (2008).
6. N.T. Kudryavtsev, T.E. Tsupak, *Zashch. Met.* **3** №4, 447 (1967).
7. S.V. Ivanov, O.O. Gerasimova, *Zashch. Met.* **33** №5, 510 (1997).
8. *New handbook of chemist and technologist. Chemical equilibrium. Solution properties* (SPb.: ANO NPO «Professional»: 2004).
9. J.N. Butler, *Ionic equilibrium: a mathematical approach* (Addison-Wesley: 1964).
10. R. Greef, R. Peat, L.M. Peter, D. Pletcher, J. Robinson, *Instrumental methods in electrochemistry* (Chichester: Ellis Horwood: 1985).
11. W. Schindler, P. Hugelmann, M. Hugelmann, F.X Kärtner, *J. Electroanal. Chem*. **522**, 49 (2002).
12. B.R. Scharifker, G. Hills, *Electrochim. Acta*. **28**, 879 (1983).
13. M. Palomar-Pardave, B.R. Scharifker, E.M. Arce, M. Romero-Romo, *Electrochim. Acta*. **50**, 4736 (2005).
14. J. Mostany, B.R. Scharifker, K. Saavedra, C. Boras, *Russian journal of electrochemistry*. **44** №6, 652 (2008).
15. A. Milchev, *Electrocristallyzation. Fundamentals of nucleation and growth*. (N.Y.: Kluwer Acad. Publ.: 2002).
16. M. Arbib, B. Zang, V. Lazarov, D. Stoychev, A. Milchev, C. Buess-Herman, *J. Electroanal. Chem*. **510**, 67 (2001).